^{177}LuPSMA-617-Therapy: Initial Experience

Kulkarni RB, Abdelrahman A, Trak J, Cengiz TB, Ghesani MV, Gavane S, Ghesani NV
Division of Nuclear Medicine, Department of Diagnostic, Interventional and Molecular Radiology
Icahn School of Medicine at Mount Sinai, New York NY

Introduction: Radioligand therapy (RLT) with ^{177}Lu-PSMA (prostate specific membrane antigen)-617 is a promising, individualised therapeutic option for mCRPC.[1] We present two of our patients treated under expanded access program with favorable response to this therapy.

Materials and methods:
Patients were selected as per the criteria outlined in the VISION trial.[2] Informed consent was obtained prior to administration of therapy.
^{177}LuPSMA-617 was administered as per the established guidelines.[2] All radiation safety protocols were followed. Post therapy scans were obtained. Patient was discharged after evaluation by Nuclear Medicine physician. Laboratory parameters were assessed every 2 weeks.

RESULTS:
Case 1: CB, diagnosed with metastatic prostate cancer in 2020, had received multiple hormonal therapies, radiation therapy to the T11 vertebra and docetaxel (May-October 2021). However, his Prostate specific antigen (PSA) continued to rise.
Radioligand therapy was therefore considered. Laboratory parameters were within acceptable limits for therapy.

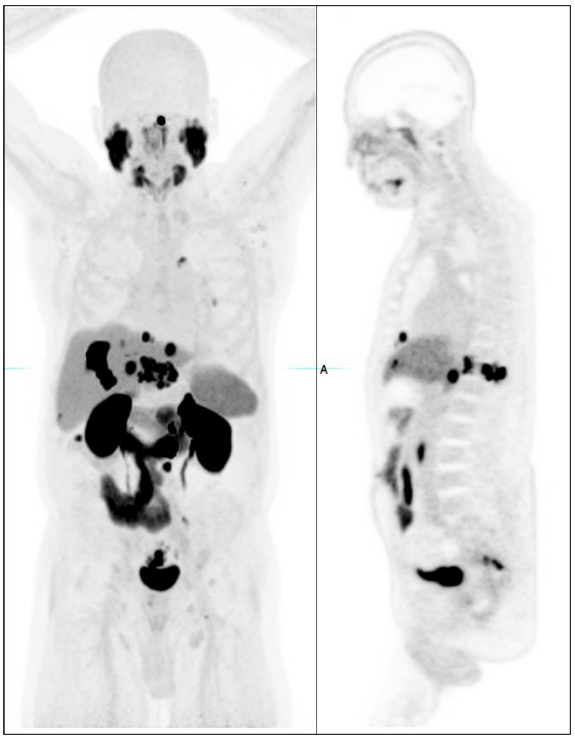

Figure 1 18FDCFPyl PET images demonstrating multiple tracer avid metastases.

He underwent therapy according to established guidelines with 200 mCi ^{177}LuPSMA-617, on 09/01/22, and 10/13/22 and underwent post therapy scan on those days (Figure 2).

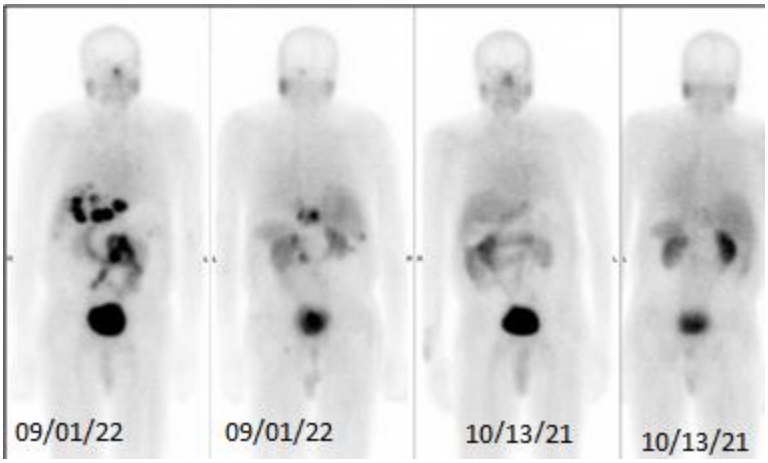

Figure 2: Post therapy scans after the first (09/01/22) and second (10/13/22) cycles. ^{177}Lu-PSMA accumulation noted in first post therapy scan, reduced uptake seen on the second scan, suggesting favorable response.

A favorable response was noted on the post therapy scans. PSA fell by 90.9% after just 2 cycles. He reported feeling well, and no untoward effects except some fatigue.

	10/10/2022	09/28/2022	09/15/2022	08/25/2022
PSA	3.1	4.2	11.4	33.2

Table 2: *CB, PSA pre and post each cycle of therapy*.

Case2: RF, a 72-year-old male, diagnosed with prostate cancer in 2012, underwent prostatectomy. Subsequently, they underwent salvage radiation to the prostate bed (2014), radiation therapy to skeletal metastases, and multiple hormonal therapies. PSA was rising despite hormonal therapies and Abiretarone. After two strokes in 2018, he was considered unfit for chemotherapy. His laboratory parameters were within limits of eligibility for therapy.
Pre therapy 18FDCFPyl PET CT demonstrated PSMA avid metastatic nodes (Figure 3).

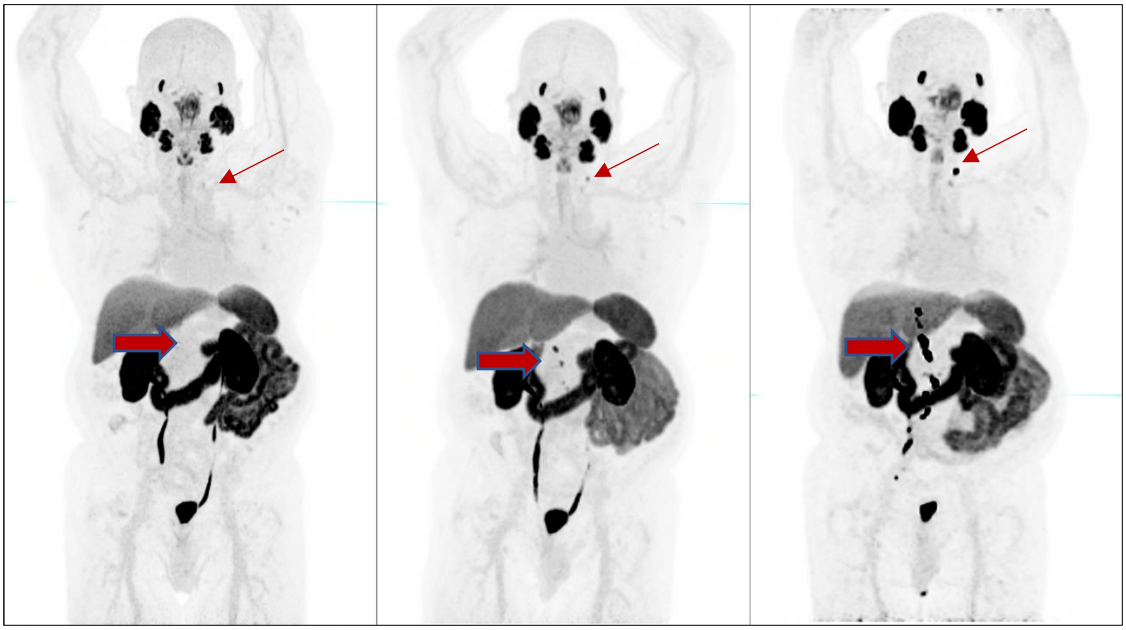

10/28/22 b. 06/02/22 c. 09/23/22

Figure 3: MIP images of 18FDCFPyl PET CT, a. pretherapy image (10/28/22) arrows point to sites of disease, after 2 cycles (06/02/22), end of treatment (09/23/22).

He received ^{177}LuPSMA-617 therapy under Investigational new drug access. He received 4 cycles of^{177}LuPSMA-617 of therapy. He did not experience any significant untoward effects immediately after therapy.

	12/29/21	1/27/22	2/9/22	3/10/22	3/23/22	5/2/22	5/25/22	6/2/22	6/30/22	7/27/22	8/17/22	08/31/22
PSA	5.82 (H)	6.73 (H)	4.27	2.30	0.95	0.18	0.09	0.07	0.04	0.02	<0.02	<0.02

Table 3: PSA levels over the course of therapy. PSA levels have fallen over the course of treatment.

Favorable response to therapy, with progressive reduction in size and PSMA uptake in the lesions were seen in the 18FDCFPyl PET CT after 2 cycles of therapy, and in the end of treatment PET CT (Figure 3a and 3b).

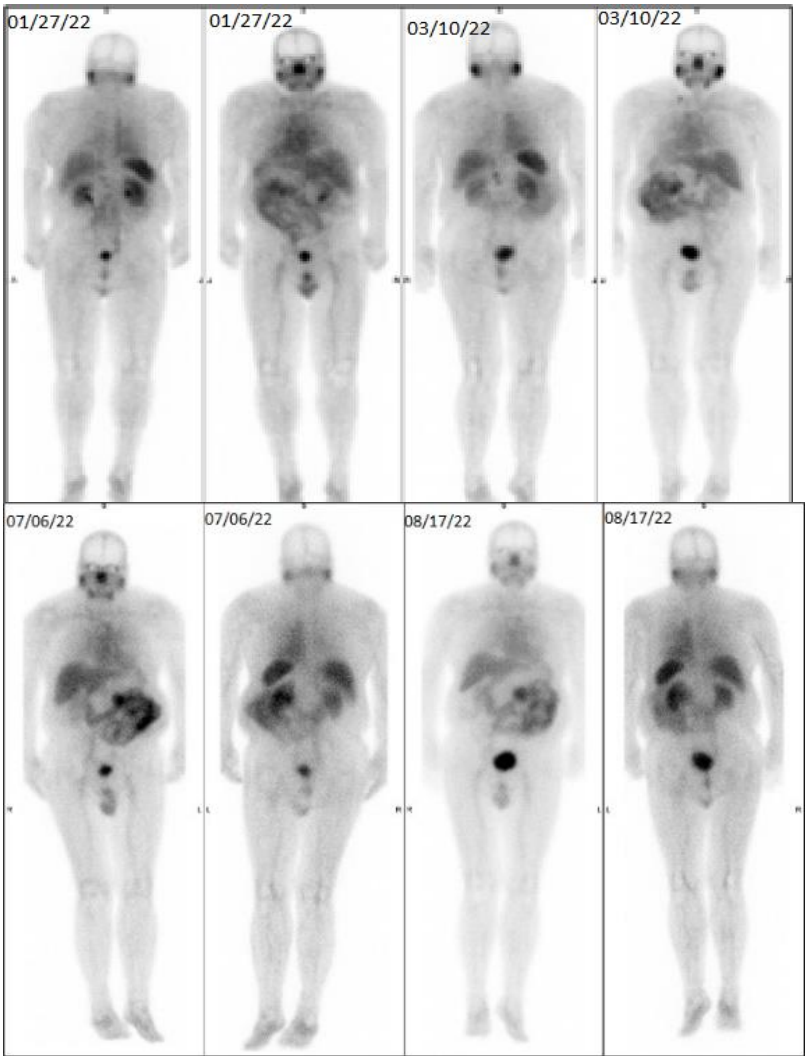

Figure 2 Post therapy scans after each cycle demonstrate favorable response to therapy.

DISCUSSION:
Both patients had favorable response to therapy, but that raises some questions.
A clinical trial comparing ^{177}LuPSMA-617 therapy and Docetaxel therapy in chemotherapy naïve mCRPC patients concluded that ^{177}LuPSMA-617 was safe and non-inferior to Docetaxel.[3] Earlier use of radioligand therapy may lead to potentially better outcomes. Also, patients like RF, unfit for chemotherapy, but with good marrow reserves would benefit.
These two patients also have predominantly soft tissue metastases. A recent study showed no relation between the site of metastasis and response to ^{177}LuPSMA-617.[4] Since this was a single center retrospectives study, further investigations into the relation between location of metastases and therapy response are warranted.

Conclusion: We aim to explore these avenues in future studies.

References:

1. Fendler, W.P., et al., *Establishing (177)Lu-PSMA-617 Radioligand Therapy in a Syngeneic Model of Murine Prostate Cancer*. J Nucl Med, 2017. **58**(11): p. 1786-1792.
2. *https://clinicaltrials.gov/ct2/show/NCT03511664*.
3. Satapathy, S., et al., *(177)Lu-PSMA-617 versus docetaxel in chemotherapy-naive metastatic castration-resistant prostate cancer: a randomized, controlled, phase 2 non-inferiority trial.* Eur J Nucl Med Mol Imaging, 2022. **49**(5): p. 1754-1764.
4. van der Sar, E.C.A., et al., *Baseline Imaging Derived Predictive Factors of Response Following [177Lu]Lu-PSMA-617 Therapy in Salvage Metastatic Castration-Resistant Prostate Cancer: A Lesion- and Patient-Based Analysis.* Biomedicines, 2022. **10**(7): p. 1575.

^{64}Cu/^{68}Ga DOTATATE-PET/CT Imaging Protocol & Workflow for Somatostatin Receptor-Positive Head & Neck Tumors: A Collaborative Approach

Graham Keir, MD; Christopher Caravella, LNMT; Ana M. Franceschi, MD, PhD; Josephine N. Rini, MD

Background:

Meningiomas and head and neck paragangliomas (HNPGLs) are the most common somatostatin receptor (SSTR) positive head and neck (H/N) tumors for which Ga-68/Cu-64 DOTATATE-PET/CT (DOTATATE-PET/CT) is performed at our institution. Due to its high sensitivity, DOTATATE-PET/CT may detect small lesions and more extensive disease than MRI, and it may more reliably differentiate residual disease from post-treatment changes. As distant metastases are uncommon with meningiomas and HNPGLs, imaging limited to the H/N may be sufficient. In addition to a shorter acquisition time, an advantage of a limited DOTATATE-PET/CT is that the PET images are more successfully fused with MRI, than vertex-to-thigh scan (VT). Brain DOTATATE-PET/MRI fusion images are especially useful for presurgical planning and for radiation treatment planning, which target DOTATATE avidity. We describe our recently introduced collaborative DOTATATE-PET/CT protocol for SSTR-positive H/N tumors and illustrate results.

Methods:

Beginning in May 2022, prior to scheduling patients with SSTR-positive H/N tumors for DOTATATE-PET/CT, we reviewed clinic notes and CT/MRI scans, and protocoled PET/CT as limited brain (B) and/or head/neck (HN), with or without VT imaging, based on lesion location and referring physician preference.

DOTATATE-PET/CT was acquired 50-60 minutes following intravenous administration of 148 MBq (4 mCi) Cu-DOTATATE or 185 MBq (5 mCi) Ga-DOTATATE using a GE Discovery 710HD. Imaging times for B, HN and VT protocols were approximately 10, 15, and 40 minutes, respectively. Acquisition and reconstruction parameters are shown in Table 1. Brain attenuation corrected PET

images were fused with previously acquired brain MRI using MIMneuro® software (version 7.1). The B and HN fused images were interpreted by a neuroradiologist and the VT images were interpreted by a nuclear medicine physician.
Following IRB approval, studies were retrospectively reviewed. A neuroradiologist classified DOTATATE activity on B/HN images as comparable (C), more extensive (E) and/or showing additional lesions (A), as compared to originally interpreted MRI. A nuclear medicine physician classified VT images, excluding H/N, as positive, if metastatic disease was present; negative, if metastatic disease was absent; and indeterminate/incidental, if unrelated findings were present.

Results:

Twelve patients (10 F, 2 M, age range of 16-69 years) with SSTR-positive H/N tumors (6 meningiomas, 4 HNPGLs [2 glomus jugulare, 1 glomus tympanicum, 1 glomus jugulotympanicum], 1 middle ear neuroendocrine adenoma, 1 pituitary carcinoma) were imaged with B (2), HN (2), B and HN (1), and B and VT (7) protocols, with either Cu-DOTATATE (11 patients) or Ga-DOTATATE (1 patient). B/HN fused images showed more extensive disease, as compared to MRI brain alone, in 3/12 patients, and additional lesions in 6/12 patients (5 meningiomas, 1 glomus jugulare paraganglioma, 1 pituitary microadenoma, 1 parathyroid adenoma, 1 suspected TMJ arthritis). For VT, 0/7 were positive, and 3/7 negative, for metastatic disease. For 4/7 scans there were indeterminate/incidental findings (adrenal adenoma, indeterminate gallbladder focus, breast lesion, 7 mm lung nodule).

Conclusions:

DOTATATE-PET/CT detected additional lesions and more extensive disease than MRI alone. By fusing PET with MRI, discrepancies were readily addressed, thereby enhancing pre-surgical assessment and radiation therapy planning, while fostering a collaborative, multi-disciplinary approach.

	PET*		CT**	
Protocol	Bed Positions	Acquisition Time (min/bed)	mA	Pitch (mm/rot)
Brain (B)	1	10	95 Fixed mA	1.375
Head/neck (HN)	3	5	50-440 Auto mA Noise Index 18.0	0.984
Vertex-to-thigh (VT)	7-8	5	30-440 Auto mA Noise Index 28.5	0.984

Table 1. DOTATATE-PET/CT protocol parameters.

*All 3D PET data was reconstructed using VUE Point FX TOF and Sharp IR. Cu-DOTATATE: 256 matrix, 3 iterations, 8 subsets, 'standard' z-axis filter, and a Gaussian post-filter of 7.0 mm FWHM.
Ga-DOTATATE: 192 matrix, 2 iterations, 24 subsets, 'standard' z-axis filter, and a Gaussian post-filter of 6.4 mm FWHM.

**All helical CT configurations utilized 120 kVp, 3.75 mm slice thickness, and a 0.8 s rotation.

POSTER # 4

SNMMI ABSTRACT:

Title: Cardiac PET to evaluate microvascular dysfunction in psoriasis.

Authors: Deepak Kalbi, MD; Adithya Hari, MD; Aspan Shokrekhuda, MD; Mark Travin, MD.

Learning Objective: Utility of cardiac PET with quantitative blood flow (QBF) to assess coronary artery dysfunction in a patient with psoriasis.

Case: A 39-year-old male smoker with diabetes and hypertension, also with psoriasis, presented with chest pain and elevated troponins. Coronary angiography showed a 70% proximal LAD thrombotic stenosis that was treated with stent placement, complicated by development of a large coronary intimal hematoma extending to the apex, necessitating temporary hemodynamic support. CTA performed 6 weeks later for recurrent symptoms showed occlusion of the LAD proximal to the stent, without significant disease of other vessels. 2 months later, to assess persistent symptoms, the patient underwent a regadenoson rest/stress N-13 ammonia positron emission tomographic (PET) imaging (10.0 mCi at stress and rest) that showed not only a large severe fixed apical defect, but also a large and severe reversible inferior wall defect. Quantitative blood flow analysis showed a globally reduced myocardial flow reserve (MFR) of 1.59, as well as reduced flow reserves in all vascular territories. Subsequent coronary angiography revealed not only an occluded distal LAD, but also a dissection of the mid-RCA. The patient underwent 2-vessel coronary bypass surgery.

Discussion: Psoriasis is a chronic systemic inflammatory disorder that has been associated with increased cardiovascular (CV) risk. Studies have shown that patients with psoriasis have both epicardial coronary artery disease (CAD) and microvascular dysfunction with vasomotor abnormalities. The fixed defect noted on the patient's PET images is secondary to the LAD infarct,

but evidence of ischemia in the inferior wall was from a new dissection of a weakened mid-RCA. Decreased flow reserve also found in the LCx territory (1.63) likely reflects abnormal microvascular dysfunction. While the patient underwent intervention for the occluded distal LAD and dissected mid- RCA, he is at increased risk from microvascular disease, and needs close follow-up with aggressive medical therapy.

Conclusion: This example establishes the utility of cardiac PET with quantitative blood flow analysis to assess the risk of epicardial and microvascular CAD in patients with psoriasis.

Reference:

- Weber B, Perez-Chada LM, Divakaran S, Brown JM, Taqueti V, Dorbala S, et al. Coronary microvascular dysfunction in patients with psoriasis. J Nucl Cardiol 2022; 29: 37-42.

POSTER # 3

The effect of thyroid probe malalignment on radio-iodine uptake measurements

Dominguez- Konicki L, Mazurek R, Siegel A

Dartmouth Hitchcock Medical Center

Lebanon, NH

Background

Location of thyroid tissue outside the thyroid bed is not uncommon. Malpositioning of a thyroid probe during a radio-iodine uptake measurement is likely to lead to inaccuracies. This may impact calculations utilized for the I-131 therapy for hyperthyroidism. We sought to determine the potential effect of incorrect positioning of the thyroid probe on uptake measurements.

Methods

We used a 300 µCi I-123 capsule in a neck phantom as a model for the thyroid gland. The probe was positioned directly above a neck phantom. Counts were recorded for one minute. The phantom was then displaced laterally by 3 cm increments up to 18 cm and counts recorded at each point. All measurements were background corrected.

We supplemented this with a calculation of the minimum lateral displacement from the probe that would result in no recordable counts using a geometric model.

Results

Our geometric calculation indicated that, at a distance of 7.5 cm, no photons would reach the probe crystal.

With the neck phantom method, at a distance of 6 cm from the probe, approximately 90% of the counts were detected by the probe. However, beyond this, the counts detected diminished drastically. At our next data point of 9 cm, less than 1% of counts were detected.

Conclusion

Ectopic or heterotopic location of the thyroid gland is unlikely to impact thyroid uptake measurements as long as the distance between the gamma probe and the thyroid is within 6 cm. This would result in an underestimation of the counts by 10% or less. Since marked ectopia of the thyroid is uncommon, such as a completely mediastinal or lingual gland, it is unlikely that malpositioning will change a diagnosis or lead to a significant miscalculation in hyperthyroidism therapy doses.

POSTER # 1

FDG-PET: Antimycobacterial treatment response to mycobacterium avium lymphadenitis

Authors: Deepak Kalbi, MD; Edgar Zamora, MD; Aspan M. Shokrekhuda, MD; Gabriel Nemzow, MD; Saeed Ghandili, MD; Renée M. Moadel, MD, MS

Background: Mycobacterium avium complex (MAC) comprises a group of nontuberculous mycobacteria (NTM) which are those other than *M. tuberculosis* and *M. leprae* [1]. These pathogens are environmental and ubiquitous, and can be found in natural water sources and soil.[2] Immunocompromised patients are at highest risk for infection, although NTM can also present in immunocompetent individuals.[3] The clinical presentation can vary widely, most often manifesting as chronic pulmonary disease, but can also present as lymphadenitis, cutaneous involvement, and systemic disease.[1]

Mycobacterium avium complex is the most common cause of NTM lymphadenitis [4]. According to an official statement from ATS/IDSA, it is treated primarily by surgical excision, with a greater than 90% cure rate. A macrolide-based regimen should be considered for patients with extensive MAC lymphadenitis or poor response to surgical therapy. In a case report by Sato et al, F18 FDG PET-CT was not only a useful diagnostic tool for the evaluation of extent and activity of disseminated MAC infection but was also more advantageous than CT and magnetic resonance imaging to assess the treatment response and time course of the disease [5].

Methods/Approach: This exhibit illustrates the use of FDG-PET/CT in evaluation of antimycobacterial treatment response in a patient with MAC lymphadenitis.

Results: The patient is an 81-year-old female with mycobacterium avium lymphadenitis diagnosed following an excisional biopsy of a left cervical lymph node. Subsequent bone marrow biopsy did not show evidence of systemic involvement. Initial FDG-PET/CT evaluation was performed with 8.8 mCi showing intensely FDG avid lymph nodes in cervical and thoracic nodal stations, and diffusely increased marrow activity. The patient started treatment with triple antibiotic therapy (azithromycin/rifampin/ethambutol). Approximately 10 months after starting therapy, follow-up FDG-PET/CT showed overall decrease in size and activity of the previously seen hypermetabolic lymph nodes, with persistent increased uptake including hilar, mediastinal, and right supraclavicular regions consistent with treatment response. Finally, a PET/CT dated 7/15/2022 showed further interval decrease in size and FDG activity of previously seen lymphadenopathy.

Conclusion: Mycobacterium avium complex is one of the most common causes of NTM lymphadenitis [4] and, like in this case, it can present in immunocompetent individuals [3]. While some patients are treated surgically, this patient was treated with antimycobacterial agents due to the widespread involvement of supradiaphragmatic lymph nodes.

FDG-PET/CT demonstrated progressive decrease in size and activity of lymphadenitis after starting therapy and, therefore, it might be a useful imaging modality for baseline imaging and treatment response evaluation in patients with MAC lymphadenitis.

References:

1. Griffith DE, Aksamit T, Brown-Elliott BA, Catanzaro A, Daley C, Gordin F, Holland SM, Horsburgh R, Huitt G, Iademarco MF, Iseman M, Olivier K, Ruoss S, von Reyn CF, Wallace RJ, Jr, Winthrop K, ATS Mycobacterial Diseases Subcommittee, American Thoracic Society, Infectious Disease Society of America. 2007. An official ATS/IDSA statement: diagnosis, treatment, and prevention of nontuberculous mycobacterial diseases. *Am J Respir Crit Care Med* 175:367–416.
2. Falkinham JO, III. 2015. Environmental sources of nontuberculous mycobacteria. *Clin Chest Med* 36:35–41.
3. Koh WJ. Nontuberculous Mycobacteria-Overview. Microbiol Spectr. 2017 Jan;5(1). doi: 10.1128/microbiolspec.TNMI7-0024-2016. PMID: 28128073.
4. Griffith, D., Aksamit, T., Brown-Elliott, B., Catanzaro, A., Daley, C., Gordin, F., Holland, S., Horsburgh, R., Huitt, G., Iademarco, M., Iseman, M., Olivier, K., Ruoss, S., von Reyn, C., Wallace, R. and Winthrop, K., 2007. An Official ATS/IDSA Statement: Diagnosis, Treatment, and Prevention of Nontuberculous Mycobacterial Diseases. *American Journal of Respiratory and Critical Care Medicine*, [online] 175(4), pp.367-416. Available at: <https://doi.org/10.1164/rccm.200604-571ST>.
5. Sato M, Hiyama T, Kaito K, Hayashi Y, Okumura T. Usefulness of F-18 FDG PET/CT in the assessment of disseminated Mycobacterium avium complex infection. Ann Nucl Med. 2009 Oct;23(8):757-62. doi: 10.1007/s12149-009-0298-5. Epub 2009 Sep 29. PMID: 19787313.

POSTER # 2

Diagnostic superiority of ^{99m}Tc-PYP SPECT/CT versus planar imaging in ATTR cardiac amyloidosis: A pilot study

William Y. Raynor, MD[1], Shelby Curren, DO[2], Kush Shah, DO[1], Anthony P. Yudd, MD, PhD[1], Jeffrey S. Kempf, MD[1]

1. Department of Radiology, Rutgers Robert Wood Johnson Medical School, 1 Robert Wood Johnson Place, MEB #404, New Brunswick, NJ 08901, USA.
2. Department of Radiology, Rutgers Health/Monmouth Medical Center, 300 2nd Avenue, Long Branch, NJ 07740, USA.

Objectives: According to American Society of Nuclear Cardiology (ASNC) guidelines for evaluation of ATTR cardiac amyloidosis with ^{99m}Tc-pyrophosphate (PYP), acquisition of both single-photon emission computed tomography (SPECT) and planar images are recommended at 1 hour. Additional imaging at 3 hours with either SPECT or planar protocols is considered optional. To assist with image interpretation and diagnosis, two metrics are suggested: heart-to-contralateral lung (H/CL) ratio and semi-quantitative visual scoring. However, there is a need to define more precise criteria for when additional imaging is necessary and how to reconcile discrepancies between the two quantitative parameters when they occur. We aimed to compare the diagnostic utility of planar imaging at 1 hour, at 3 hours, and SPECT/CT at 1 hour using the quantitative methods described by ASNC guidelines to determine the best method to diagnose ATTR cardiac amyloidosis.

Methods: Thirty-three patients with suspected ATTR cardiac amyloidosis underwent planar imaging with anterior, left anterior oblique, and left lateral views at 1 and 3 hours after administration of 15 mCi ^{99m}Tc-PYP. SPECT/CT images were also acquired at the 1-hour time point. As suggested by ASNC, H/CL ratios were measured on planar images only and classified as not suggestive (<1.0), equivocal (1.0-1.5), and strongly suggestive (>1.5). Similarly, semi-quantitative visual scores were recorded as not suggestive (grade 0), equivocal (grade 1), and strongly suggestive (grade 2 and 3).

Results: The overall diagnostic impressions for 33 patients resulted in 5 studies positive for ATTR cardiac amyloidosis, 2 equivocal studies, and 26 negative studies. SPECT/CT visual scoring was concordant with the final impression in all 5 positive cases and in 25 out of 26 negative cases (with 1 equivocal score being recorded). Planar imaging visual scores were similarly concordant in all 5 positive cases at both time points; however, among negative studies, 19/26 (73%) scores were equivocal or false positive at 1 hour, decreasing to 8/26 (31%) at 3 hours. H/CL ratios were equivocal in 2/5 positive studies at 1 hours, decreasing to 1 equivocal ratio at 3 hours. All 26 H/CL ratios were equivocal or false positive among negative studies at 1 hour, decreasing to 24/26 discordant H/CL ratios at 3 hours.

Conclusion: Visual scoring applied to all methods of imaging assessed appeared sufficiently sensitive to identify uptake consistent with ATTR cardiac amyloidosis. However, only SPECT/CT demonstrated the degree of specificity necessary to discriminate between myocardial uptake and blood pool activity. Among the planar imaging time points, 3 hour imaging decreased equivocal findings and was more consistent with the final impression using both visual scoring

and H/CL ratio. Therefore, visual scoring of SPECT/CT images obtained at 1 hour appears optimal for diagnosing ATTR cardiac amyloidosis with ^{99m}Tc-PYP, followed by visual scoring of 3 hour planar images in instances where SPECT/CT is not feasible.

POSTER # 5

Cardiac Amyloidosis Scanning with Integrative Use of Planar and SPECT/CT: Pearls and Pitfalls

Authors

Adithya Hari, MD; Deepak Kalbi, MD; Saeed Ghandili, MD; Aspan Shokrekhuda, MD; Mark Travin, MD

Division of Nuclear Medicine
Department of Diagnostic Radiology
Montefiore Medical Center and the Albert Einstein College of Medicine
1695A Eastchester Rd, The Bronx, NY, 10461

Correspondence

Adithya Hari, MD
ahari@montefiore.org
Tel (718) 405-8462 / Fax (718) 824-0625
Montefiore Medical Center
1695A Eastchester Rd, The Bronx, NY, 10461

Abbreviations

Cardiac amyloidosis; ATTR; Scintigraphy; PYP Imaging; Heart Failure.

Conflict of Interest

None of the authors have any conflicts of interest to disclose nor have received any type of financing related to this manuscript.

Background

Cardiac amyloidosis is an underdiagnosed cause of heart failure, precipitated by deposition of improperly metabolized misfolded proteins. The main forms of cardiac amyloidosis are transthyretin type (ATTR), which can be either wild type (ATTRwt) or hereditary (ATTRv), caused by mutations of *TTR* gene, and light chain type (AL), that is usually seen as a part of plasma cell dyscrasias. Demonstration of these deposited fibrils histologically by an endomyocardial biopsy has been the standard for diagnosing cardiac amyloidosis[1].

Bone seeking radiopharmaceuticals, such as technetium 99m labelled pyrophosphate (^{99m}Tc-PYP), 3,3-diphosphono-1,2-propanodicarboxylic acid (^{99m}Tc-DPD), and hydroxymethylene diphosphonate (^{99m}Tc-HMDP) have been shown to have a high sensitivity and specificity, the mechanism thought to be binding to the microcalcifications within the amyloid fibrils[2]. Standard protocol involves IV administration of ~20mCi of ^{99m}Tc-PYP followed 2-3 hours later (1 hour optional) with planar and SPECT imaging of the chest, the latter preferably with CT if available[3]. SPECT/CT allows direct visualization of myocardial tracer uptake.

Gilmore et al, reported that bone scintigraphy was 99% sensitive and 86% specific for cardiac ATTR with false positive cases almost exclusively from AL amyloidosis[4]. To approach a 100% positive predictive value, along with appropriate patient selection (older adults with unexplainable heart failure and suggestive EKG, echocardiographic, or cardiac MRI abnormalities), auxiliary biochemical testing with serum and urine electrophoresis needs to be performed[3]. In addition to supplemental testing and instrumentation errors, the interpreting reader should be aware of the other clinically significant cardiac and extra-cardiac findings of the bone tracers in this targeted exam.

Methods/Approach

This image-rich case-based educational exhibit will review the pertinent positive and negative findings of cardiac amyloidosis scanning.

Results

Illustrative examples are provided for several clinical scenarios describing various pearls and pitfalls of cardiac amyloidosis imaging. These include examples of expected findings in true-positive, true-negative, false positive and equivocal scans. Attention to reporting the extra-cardiac findings will also be made.

Conclusion

Cardiac amyloidosis imaging is a well proven modality for noninvasive diagnosis of ATTR amyloidosis. While initial amyloid deposition is asymptomatic, the condition eventually leads to restrictive cardiomyopathy and heart failure. Prompt diagnosis by careful image interpretation translates to better patient outcomes.

References:

1. Ruberg FL, Berk JL. Transthyretin (TTR) cardiac amyloidosis. Circulation. 2012; 4;126(10):1286-300.
2. Stats MA, Stone JR. Varying levels of small microcalcifications and macrophages in ATTR and AL cardiac amyloidosis: implications for utilizing nuclear medicine studies to subtype amyloidosis. Cardiovascular Pathology. 2016;25(5):413-7.
3. Dorbala S *et al*. Addendum to ASNC/AHA/ASE/EANM/HFSA/ISA/SCMR/SNMMI expert consensus recommendations for multimodality imaging in cardiac amyloidosis: Part 1 of 2—evidence base and standardized methods of imaging. Journal of Nuclear Cardiology. 2021;28(4):1769-74.
4. Gillmore JD, Maurer MS, Falk RH, Merlini G, Damy T, Dispenzieri A, Wechalekar AD, Berk JL, Quarta CC, Grogan M, Lachmann HJ. Nonbiopsy diagnosis of cardiac transthyretin amyloidosis. Circulation. 2016;133(24):2404-12.

POSTER # 6

Hyperparathyroidism: The Importance and Unique Role of Nuclear Medicine

Matteen Hakim, MD, Ronald Rosenberg MD, and Prasanta Karak MD

Background:

Hyperparathyroidism is a common illness affecting many patients, and a very high proportion of the affected patients have hyperparathyroidism secondary to a parathyroid adenoma. Many patients even have multiple parathyroid adenomas. The treatment for hyperparathyroidism secondary to a parathyroid adenoma involves surgical removal of the diseased parathyroid gland(s). In order to decrease the extent of surgical exploration of the neck, surgeons rely on nuclear medicine techniques to guide the surgery. Anatomical imaging has not been able to reliably pinpoint parathyroid adenomas compared to the scintigraphic techniques provided by nuclear medicine. In addition to pre-operative use, radiotracers are also used intraoperatively by surgeons to pinpoint exactly where their incision should be to minimize surrounding damage.

Methods:

This presentation is meant as an educational exhibit on the workup of hyperparathyroidism from a scintigraphic perspective. Information was obtained via literature review and our experience over the last several years at Hartford Hospital. Subsequently, imaging from multiple cases of hyperparathyroidism were reviewed as a case series, each obtained at Hartford Healthcare institutions. The clinical data was obtained via chart review to correlate the imaging findings with surgical and pathologic findings.

Results:

Imaging was obtained with the use of pinhole collimators after administration of ^{99m}Tc-Sestamibi and ^{123}I (dual tracers). Subtraction images were then obtained. In many cases, SPECT/CT was also performed. Some cases were also repeated after a delay to have a dual time point imaging. Examples of different pathologies with appropriate imaging as well as surgical and pathological correlation will be displayed.

Conclusions:

In the workup of hyperparathyroidism, nuclear medicine plays an indispensable role in identifying parathyroid adenomas and decreasing surgical complications by guiding operative management. In our institution, we have found the most success with the use of dual isotope imaging with pinhole collimators and subtraction for diagnosis of parathyroid adenomas. SPECT/CT was less useful for many of the analyzed cases as the adenomas were not able to be identified on the anatomic imaging. Intraoperatively, ^{99m}Tc-Sestamibi is used invariably by surgeons to localize the suspected adenoma to minimize the incision size and extent. The ability to not only identify the problematic parathyroid glands preoperatively but also pinpoint the gland intraoperatively results in a collaborative workflow where nuclear medicine is integral to the management of such patient.

POSTER # 7

Proposed Applications of FDG-PET/CT in Patients Referred for Yttrium-90 Radioembolization

Victoria Kim, MD[1,2], William Raynor[1,3], MD, Abass Alavi, MD[1]

1. Department of Radiology, Hospital of the University of Pennsylvania, 3400 Spruce Street, Philadelphia, PA 19104, USA.
2. Department of Radiology, Rutgers Health/Monmouth Medical Center, 300 2nd Avenue, Long Branch, NJ 07740, USA.
3. Department of Radiology, Rutgers Robert Wood Johnson Medical School, 1 Robert Wood Johnson Place, MEB #404, New Brunswick, NJ 08901, USA.

Objective:

We aim to discuss the utilization of FDG-PET/CT in patients referred for yttrium-90 therapy, including patients with primary hepatocellular carcinoma (HCC) as well as metastatic disease to the liver.

Background:

FDG-PET/CT has played a major role in cancer staging for operative versus non-operative/palliative planning along with assessing treatment response and detecting cancer recurrence. Although many liver cancers are managed with surgical resection, nonoperative candidates or those with metastatic disease to the liver often rely on other forms of treatment. Interventional oncology has continued to become a major contributor in the multi-disciplinary clinical management of multiple cancers, many of which include tumors involving the liver. With the progress in minimally invasive procedures including yttrium-90 radioembolization, patients with primary liver cancer and those with metastatic disease have been able to receive personalized intervention tailored to the extent and aggressiveness of their disease. In order to predict and evaluate the effectiveness of yttrium-90 radioembolization, FDG-PET/CT has been proposed to be completed pre- and post-procedure, respectively.

Clinical Applications:

Following yttrium-90 radioembolization, FDG-PET/CT can identify treatment response and predict patient survival more accurately compared to CT. Due to the variability of tumor grade in HCC, the pattern of FDG uptake can also be quite variable prior to treatment. Nevertheless, recent data suggests that pretreatment FDG uptake of the tumor is associated with greater progression free survival, despite these lesions being more metabolically active. Additionally, FDG-PET/CT findings can change the management in patients with hepatic metastasis. This has specifically been noticed in cases of primary colorectal cancer. By visualizing site of disease activity throughout the body with high sensitivity, FDG-PET/CT has the potential to identify new extrahepatic disease not previously seen on other modalities. In some cases, the new information offered by PET was critical in determining the necessity of yttrium-90 radioembolization.

Conclusion:

The utilization of FDG-PET/CT in patients referred for yttrium-90 radioembolization has the potential to change management in patients with primary liver cancer in addition to those with

metastatic disease to the liver. However, large prospective data following the currently available preliminary studies are needed. These studies should clarify which patients would benefit the most form either pre- or post-procedure FDG-PET/CT and the optimal times to perform imaging.

POSTER # 8

The Utility Of Early Gallium-67-Citrate Scanning In The Evaluation Of Atypical Thyroiditis: A Case Report

Authors: Surita Banerjee, MD; Adithya Hari, MD; Deepak Kalbi, MD and Kwang Chun, MD.

Disclosures: The above authors have no financial disclosures to declare.

Address for correspondence

Kwang Chun, MD

Department of Radiology, Division of Nuclear Medicine

Montefiore Medical Center/ Albert Einstein College of Medicine, Bronx, NY 10467

Phone number: (+1) 248-819-2321

Chunk@montefiore.org

Learning Objective: To reiterate the usefulness of ^{67}Gallium-citrate in a patient with acute thyroiditis, who presented with FUO.

Case: A 42-year-old male with unremarkable medical history presented to the hospital with fever associated with chills and sore throat. Initial work-up showed leukocytosis with no cultures identified in the blood along with negative HIV, AFB and respiratory pathogen panel. CT scan of chest with contrast revealed right lung micronodules with cervical and small interspread concentric lymphadenopathy. The patient then developed right neck tenderness. Thyroid panel showed suppressed thyroid-stimulating hormone (TSH < 0.05) and free thyroxine (FT4 >6.0). Antithyroperoxidase and antithyroglobulin antibodies as well anti-TSH receptor antibodies, were negative. Ultrasound of neck showed heterogeneously appearing thyroid. Initially, thyroid uptake and scan was considered, but later scanning with ^{67}Gallium-citrate scan was planned and performed. ^{67}Gallium-citrate whole body scan demonstrated focal increased radiotracer uptake in the right thyroid lobe, suggestive of inflammatory/neoplastic process. Though no nodule was seen on the ultrasound, based on the focality of the scan, a decision was biopsy the focal lesion to rule out malignancy. Pathology revealed numerous dispersed and clustered epithelioid histiocytes, numerous multinucleated giant cells and colloid, consistent with subacute granulomatous (De Quervian's) thyroiditis. The patient was discharged on a short course of NSAIDs. The repeat thyroid function tests 3 months later were normal.

Discussion: Subacute or De Quervain's thyroiditis usually occurs after an upper respiratory tract infection (in the case presented there was no evidence of such disease) and presents with a painful and tender goiter that is associated with general malaise and possible fever. Thyroid pain or tenderness is noted in ~75 % of the patients[1]. The diagnosis is usually made clinically and is supported by the biochemical findings of hyperthyroidism and the suppressed ^{123}I or ^{99m}Tc uptake by the thyroid gland. However, since the patient had recent exposure to iodinated contrast, it was deemed not suitable for the patient. ^{67}Ga- citrate is an iron analogue that is found to be concentrating in scintigraphy is an established imaging modality in patients with FUO, because it can detect both acute and chronic inflammatory conditions and/or neoplasms[3]. Increased ^{67}Ga-citrate uptake by the thyroid gland may be due to neoplastic involvement or due to benign causes such as acute suppurative thyroiditis, autoimmune thyroiditis, silent thyroiditis, amiodarone-induced hyperthyroidism, Graves' disease, and even benign adenomatous goiter.

Conclusion: For a patient with ambiguous clinical symptoms like FUO and neck pain, this case exemplifies the utility of early ^{67}Ga-citrate scanning in guiding further patient management.

References:

1. Daniels GH. Atypical subacute thyroiditis: preliminary observations. Thyroid. 2001;11(7):691-5.
2. Knockaert DC, Mortelmans LA, De Roo MC, Bobbaers HJ. Clinical value of gallium-67 scintigraphy in evaluation of fever of unknown origin. Clinical Infectious Diseases. 1994;18(4):601-5.

POSTER # 9

Title

Cardiac allograft vasculopathy following cardiac transplantation - an enigma unshrouded by ^{13}N-Ammonia Positron Emission Tomography with Quantitative Blood Flow Analysis.

Correspondence

Aspan Meherzad Shokrekhuda

ashokrekhu@montefiore.org

Tel (718) 920-5013 / Fax (718) 920-2629

Montefiore Medical Center and the Albert Einstein College of Medicine

Division of Nuclear Medicine, Department of Radiology

111 E 210Th St

The Bronx, NY, 10467

Authors

Aspan M. Shokrekhuda, MD; Deepak Kalbi, MD; Adithya Hari, MD; Mark Travin, MD

SNMMI Abstract

Objective: Advantage of ^{13}N-Ammonia Positron Emission Tomography with Quantitative Blood Flow Analysis (^{13}N-Ammonia PET with QBF) in non-invasive early detection of cardiac allograft vasculopathy (CAV).

Background: Cardiac allograft vasculopathy (CAV) is a major cause of chronic graft failure post cardiac transplant (1). The characteristic finding of CAV is concentric fibrous intimal hyperplasia of the coronary vessels (2). The overall prevalence of CAV at 1-, 5- and 10-years post transplantation is 8%, 29% and 47% (3). Clinical symptoms are typically absent in CAV; with heart failure, myocardial infarction, or sudden cardiac death being the initial presentation. Therefore, screening studies are extremely important for detecting CAV. Invasive coronary angiography (CAG) is the gold standard; however, it lacks sensitivity at an early stage with many patients not having angiographically visible abnormalities (3,4). This is due to the disease involving the coronary walls and the microvasculature, often requiring further invasive intravascular ultrasound (IVUS) or optical coherence tomography (OCT) to detect. Positron emission tomography (PET), with quantitative blood flow analysis imaging is noninvasive and is essential for detection of microvascular abnormalities based on decreased coronary flows (5,6).

Method: This exhibit will illustrate a compelling case of CAV status post cardiac transplantation initially found on Regadenoson ^{13}N-Ammonia positron emission tomography with quantitative blood flow analysis (^{13}N-Ammonia PET with QBF) two years following transplantation. Thereafter, worsening of findings on a 4-year post-transplant ^{13}N-Ammonia PET will be illustrated.

Results: A 40-year-old morbidly obese and hypertensive male, status post cardiac transplantation due to nonischemic cardiomyopathy, initially presented with a normal CAG one year following transplantation. A subsequent ^{13}N-Ammonia PET with QBF 2-year post-transplant demonstrated normal conventional image displays with abnormal blood flow values, suggestive of CAV. His angiography at the time was normal. The patient's ^{13}N-Ammonia PET 4-year post-transplant found worsening of coronary blood flow values, with ensuing coronary angiography confirming tapering of distal coronary vessels, indicative of CAV.

Summary: The ^{13}N-Ammonia PET with QBF was essential for detection of early CAV 2-year post-transplantation based on abnormal coronary blood flow values despite normal coronary angiography, as CAG lacks sensitivity at detecting CAV at an early stage (3,4). Furthermore, a ^{13}N-Ammonia PET with QBF 4-year post-transplantation found further abnormal coronary blood flow values, suggesting worsening of CAV compared to the previous scan. This was further confirmed with tapering of blood vessels on a subsequent CAG, which is known to be an anatomic abnormality characteristic of CAV (7). The findings presented here on ^{13}N-Ammonia PET imaging with QBF highlight a powerful non-invasive technique for detecting early CAV. Further studies may show potential ability of perfusion PET with QBF for guiding current therapies and help develop new ones to effectively treat CAV and thereby prevent adverse patient outcomes.

References:

1. Khush KK, Cherikh WS, Chambers DC, et al. The International Thoracic Organ Transplant Registry of the International Society for Heart and Lung Transplantation: Thirty-sixth adult heart transplantation report - 2019; focus theme: Donor and recipient size match. J Heart Lung Transplant 2019; 38:1056.

2. Ramzy D, Rao V, Brahm J, Miriuka S, Delgado D, Ross HJ. Cardiac allograft vasculopathy: a review. Can J Surg. 2005 Aug;48(4):319-27.

3. Gustafsson, F. (2022). Heart transplantation: Clinical manifestations, diagnosis, and prognosis of cardiac allograft vasculopathy. UpToDate. Retrieved 2022, from https://www.uptodate.com/contents/heart-transplantation-clinical-manifestations-diagnosis-and-prognosis-of-cardiac-allograft-vasculopathy.

4. Costanzo MR, Naftel DC, Pritzker MR, et al. Heart transplant coronary artery disease detected by coronary angiography: a multi-institutional study of preoperative donor and recipient risk factors. Cardiac Transplant Research Database. J Heart Lung Transplant 1998; 17:744.

5. Pampaloni MH, Shrestha UM, Sciammarella M, Seo Y, Gullberg GT, Botvinick EH. Noninvasive PET quantitative myocardial blood flow with regadenoson for assessing cardiac allograft vasculopathy in orthotopic heart transplantation patients. J NuclCardiol 2017; 24:1134-44.

6. Chih S, Chong A, Erthal F, et al. PET Assessment of Epicardial Intimal Disease and Microvascular Dysfunction in Cardiac Allograft Vasculopathy. J Am Coll Cardiol. 2018 Apr, 71 (13) 1444–1456.

7. Clarke, B., & Khush, K. (2012). Cardiac Allograft Vasculopathy: An ongoing challenge in the care of heart transplant recipients. Cardiac Transplantation. 2012 Feb.

POSTER # 10

Title

Pseudomyogenic hemangioendothelioma on ^{18}F-FDG PET/CT: A cryptic locally aggressive neoplasm with distinctive manifestations.

Correspondence

Aspan Meherzad Shokrekhuda

ashokrekhu@montefiore.org

Tel (718) 920-5013 / Fax (718) 920-2629

Montefiore Medical Center and the Albert Einstein College of Medicine

Division of Nuclear Medicine, Department of Radiology

111 E 210Th St

The Bronx, NY, 10467

Authors

Aspan M. Shokrekhuda, MD; Edgar Zamora, MD; Deepak Kalbi, MD; Kwang J. Chun, MD; Renee M. Moadel, MD

SNMMI Abstract

Objective: Familiarize the reader with the pathophysiology, clinical behavior, and imaging manifestations of pseudomyogenic hemangioendothelioma on ^{18}F-FDG PET/CT and correlative radiologic studies.

Background: Pseudomyogenic hemangioendothelioma (PMHE) is a rare vascular neoplasm most commonly manifesting in cutaneous and subcutaneous tissues of the upper and lower extremities (1), with bone involvement in approximately 14% of patients (2). It often presents with multifocal regional disease, follows an indolent course, and rarely metastasizes distally. Histopathologically, PMHE mimics epithelioid sarcoma with marked fibroplasia, although some dissimilarities are found on immunohistochemistry (3). The diagnosis of PMHE, therefore, can be complicated by nonspecific clinical manifestations and equivocal microscopy (4). On imaging studies, PMHE usually manifests as well circumscribed lobulated lesions and is often detected incidentally. Cross-sectional imaging studies are particularly useful for evaluation of soft tissue plane involvement, although imaging manifestations can be discordant among different modalities. Computed tomography can show osseous involvement as expansile osteolytic lesions, while soft tissue lesions appear as nonspecific lobulated densities. On Magnetic Resonance Imaging (MRI), these lesions can show variable high signal intensity on T2 weighted images with homogeneous to slightly heterogeneous contrast enhancement on T1 images with contrast. A few case studies have described the appearance of PMHE on ^{18}F-FDG PET/CT as intensely avid multifocal lesions that can be limited to a region (e.g., lower extremity) (5).

Method: This image-rich educational exhibit will review the pathophysiology and most common manifestations of PMHE. It will present a case of multicentric PMHE on ^{18}F-FDG PET/CT with

histopathology and correlative findings on MRI. Additionally, the exhibit will review the interval follow up on ^{18}F-FDG PET/CT post treatment with everolimus.

Results: A 19-year-old woman presented to our institution with a tender right thigh soft tissue mass. MRI findings suggested a vascular malformation in the anterolateral right thigh musculature with noncontiguous foci of disease in the middle to distal thigh. Sclerotherapy failed to alleviate her pain, and a subsequent open biopsy revealed PMHE. The patient underwent an ^{18}F-FDG PET/CT with 9.2 millicuries revealing numerous foci of intense activity in the right thigh which had not been evidenced on other conventional imaging studies. Subsequently, the patient began therapy with everolimus for her PMHE and trimethoprim-sulfamethoxazole for P. jirovecii prophylaxis. On her subsequent ^{18}F-FDG PET/CT, the patient was found to have interval decrease in the size, number, and intensity of the FDG-avid lesions.

Conclusion: PMHE are rare vascular neoplasms with unusual clinical and imaging manifestations (2,3). Conventional imaging studies can be non-specific and the diagnosis of PMHE requires tissue biopsy with immunohistochemical staining (3). In this case, initial MRI findings suggested a vascular malformation in the anterolateral right thigh, eventually requiring an open biopsy which revealed PMHE. However, despite the MRI findings and tissue biopsy, the extent of the disease was not unearthed until the initial ^{18}F-FDG PET/CT (5). Additionally, upon treatment with everolimus, there was interval decrease in disease extent visualized on the subsequent ^{18}F-FDG PET/CT. This case accentuates ^{18}F-FDG PET/CT can be a sensitive diagnostic modality useful in staging, metastatic evaluation, and surveillance for PMHE.

References:

1. Choi, J. H., & Ro, J. Y. (2020). The 2020 who classification of tumors of soft tissue: Selected changes and new entities. Advances in Anatomic Pathology, 28(1), 44–58.

2. Otani S, Nakayama R, Sekita T, Hirozane T, Asano N, Nishimoto K, et al. Pseudomyogenic hemangioendothelioma of bone treated with denosumab: a case report. BMC Cancer. 2019; 19:1-6.

3. Cd, L. HJ, Fletcher. Pseudomyogenic hemangioendothelioma: a distinctive, often multicentric tumor with indolent behavior. The American journal of surgical pathology. 2011;35.

4. Al-Qaderi A, From the Department of Pathology M, Forensic Medicine, Mansour AT, From the Department of Pathology M, Forensic Medicine. Pseudomyogenic Hemangioendothelioma. Archives of Pathology & Laboratory Medicine. 2021; 143:763-7.

5. Liu Y. Pseudomyogenic Hemangioendothelioma: Distinctive FDG PET/CT Findings with Numerous Multilayer Lesions in a Single Distal Extremity. Clinical nuclear medicine. 2020;45.

6. Joseph J, Wang WL, Patnana M, et al. Cytotoxic and targeted therapy for treatment of pseudomyogenic hemangioendothelioma. Clin Sarcoma Res. 2015; 19:22.

POSTER # 11

Title: Dosimetry of 177Lu-DOTATATE in a patient on home hemodialysis with bone marrow toxicity.
Authors: Saeed Ghandili, MD; Deepak Kalbi, MD; Na Song, Ph.D.; Renée M. Moadel, MD, MS

Background: 177 Lu-DOTATATE-octreotide therapy is a novel treatment for patients with unresectable metastatic neuroendocrine tumors (NET), which is an effective therapy option with a low toxicity rate. We report bone marrow dosimetry for a patient with an unresectable recurrent metastatic neuroendocrine tumor. After one treatment with 177Lu-DOTATATE, the patient had grade 2 thrombocytopenia post-treatment, which subsequently resolved.

Method: The patient is a 46-year-old female with end-stage renal disease due to a prior left nephrectomy due to a malignancy and a right kidney neoplasm. The patient is on home hemodialysis utilizing the VersiHD (Nxstage Medical Inc.) system. She also has a stage III small bowel ileal low-grade neuroendocrine tumor with a history of resection and recurrence with unresectable liver metastasis and lymphadenopathy. She was on Lanreotide for two years with progression of disease on gallium-68 DOTATATE PET/CT with multiple lesions within the liver, paravertebral lymph nodes, and pancreas. Labs showed rising Chromogranin A level. Based on the literature on 177Lu-DOTA-octreotate in patients on dialysis, 200 mCi of 177Lu-DOTA-octreotate treatment was administered; the patient was advised for home dialysis on the evening of therapy, the day after therapy, and three days after therapy. She was advised to bring the tubing and cartridge post-hemodialysis to radiation safety for safe radioactive waste disposal. Whole-body planar images were acquired 24, 48, and 120 hours after therapy. SPECT/CT of the chest and abdomen was acquired at 24 hours to rescale the organs' time activity curve based on data extracted from the geometric mean of planar images for more accurate dosimetry. Regions of interest were drawn on planar and SPECT/CT images over organs with high uptake, the spleen, liver, and heart, using Hermes software. Bone marrow and kidneys are the primary dose-limiting organs for 177Lu-DOTAnd-octreotate treatment; however, the remaining kidney was nonfunctioning. Bone marrow dose was calculated using the high uptake organs and body remainder as the source organs: QPlanar method was applied to calculate the cumulated activity of spleen, liver, heart, and body remainder; MIRDcal_v1.1 internal dose calculation software was used for dosimetry calculation.

Results: Only minimal biological elimination was observed, indicating the home dialysis machine did not adequately filter 177Lu-DOTA-octreotate. The estimated absorbed dose of bone marrow was 2.07 Gy, and the maximum tolerated absorbed dose for bone marrow over multiple treatment cycles is 2 Gy. This was due to the limited biological elimination of this patient. This patient had grade 2 thrombocytopenia which resolved three months after therapy, and Chromogranin A level decreased from 14935 ng/ml to 2848 ng/ml 6 months after. The patient was not advised to undergo further therapy with 177Lu-DOTA-octreotate due to achieving the maximum bone marrow tolerated dose.

Conclusion: For patients on a home dialysis system, the 177Lu-DOTA-octreotate therapy dose may not be adequately filtered; a reduced treatment dose should be administered during the first cycle to avoid bone marrow toxicity. Dosimetry should be considered in a home dialysis patient, and the dose of the following treatment cycles can be adjusted accordingly.

POSTER # 12